CHAPTER 4

RESULTS AND DISCUSSION

4.1 Variation of Coefficient of drag force with back slant angle (α) at U_∞= 30m/s

Slant Angle (α)	Coefficient of Drag force (C_d)
10°	0.2873
12.5°	0.2886
15°	0.2928
20°	0.2962
25°	0.2984
30°	0.3145
35°	0.30008

TABLE 4.1 Variation of Coefficient of drag force with back slant angle (α)

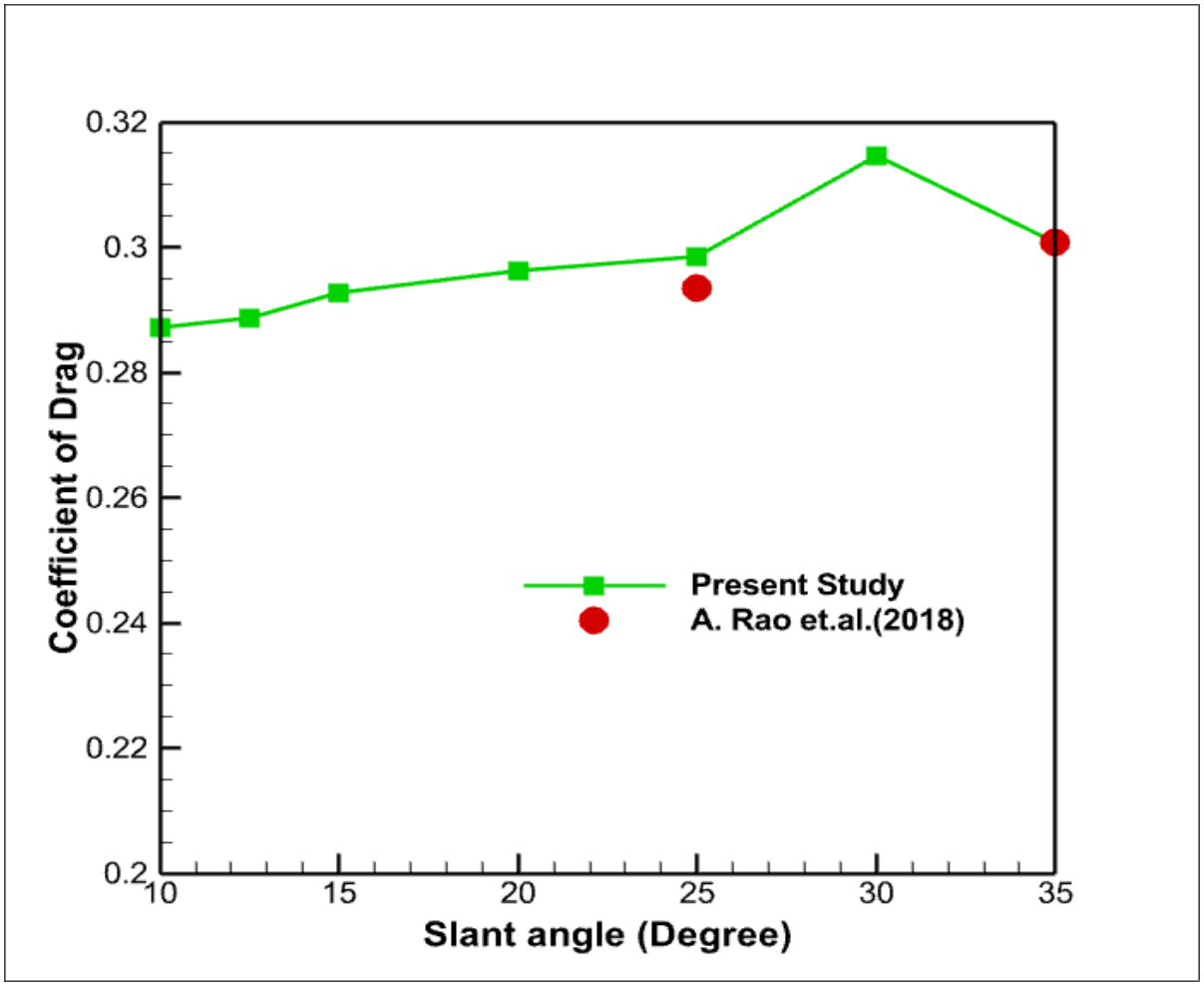

Fig 4.1 Graph of Coefficient of drag with slant angle

The drag coefficient of Ahmed body is highly depends on the back slant angle. The same trend of drag coefficient was observed by Ahmed, S. R. et.al in research article "Some Salient Features of the Time Averaged Ground Vehicle Wake".When 12.5° <α< 30° , the drag coefficient increases with the back slant angle as the flow becomes much more 3 dimensional and longitudinal vortices becomes much more stronger. In this region the flow remains attached to the back slant surface**.** When α = 30° the flow at the top of the roof separates and it reattaches on the slant surface and hence forming a separation bubble at the slant surface. The separation bubble at the slant surface causes the pressure to drop at the slant surface region and provide strengths to the longitudinal vortices. This is the main cause of why the aerodynamic drag shoot up at the α = 30° .In regime 3rd where α > 30°˚,the separated flow at the top of the roof of Ahmed body is no longer to reattach on the slant surface hence there will be overall constant pressure at the slant surface which results

decrease of aerodynamic drag and also the strength of longitudinal vortices is also decrease in this regime

4.2 Variation of velocity in x direction along the lines shown below

At U_∞ =40 m/s, α = 35°

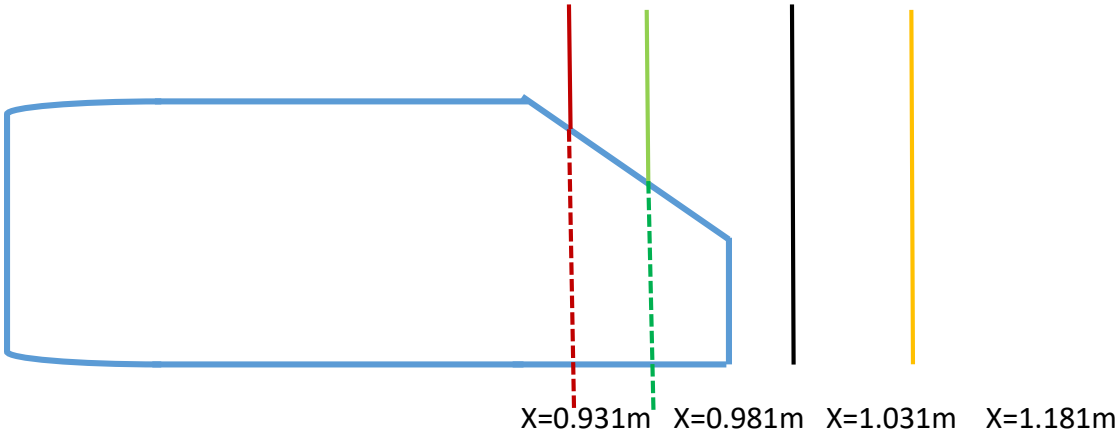

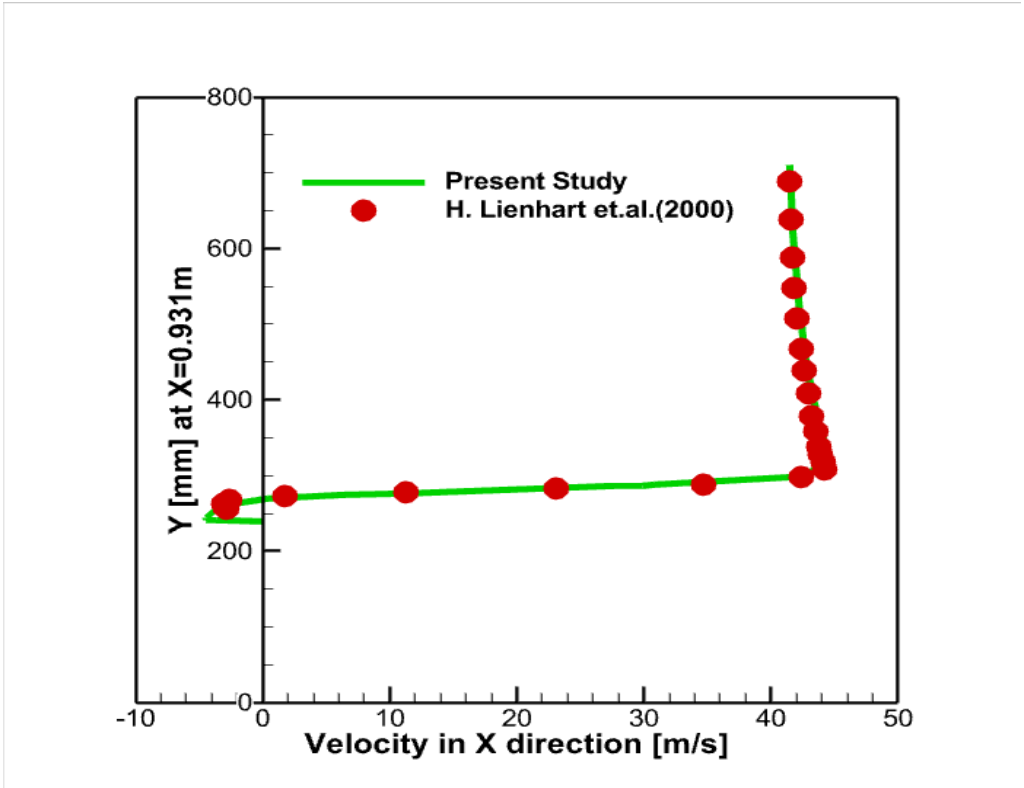

(a)

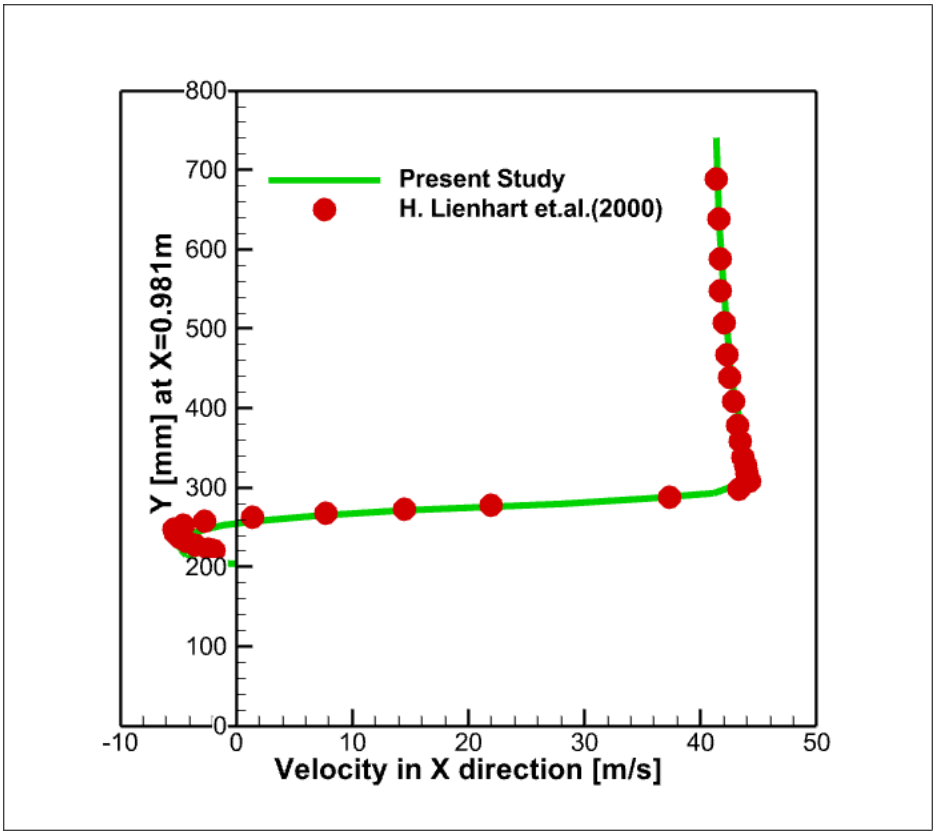
Present Study
H. Lienhart et.al.(2000)
Y [mm] at X=0.981m
Velocity in X direction [m/s]
800
700
600
500
400
300
200
100
0
-10
0
10
20
30
40
50

(b)

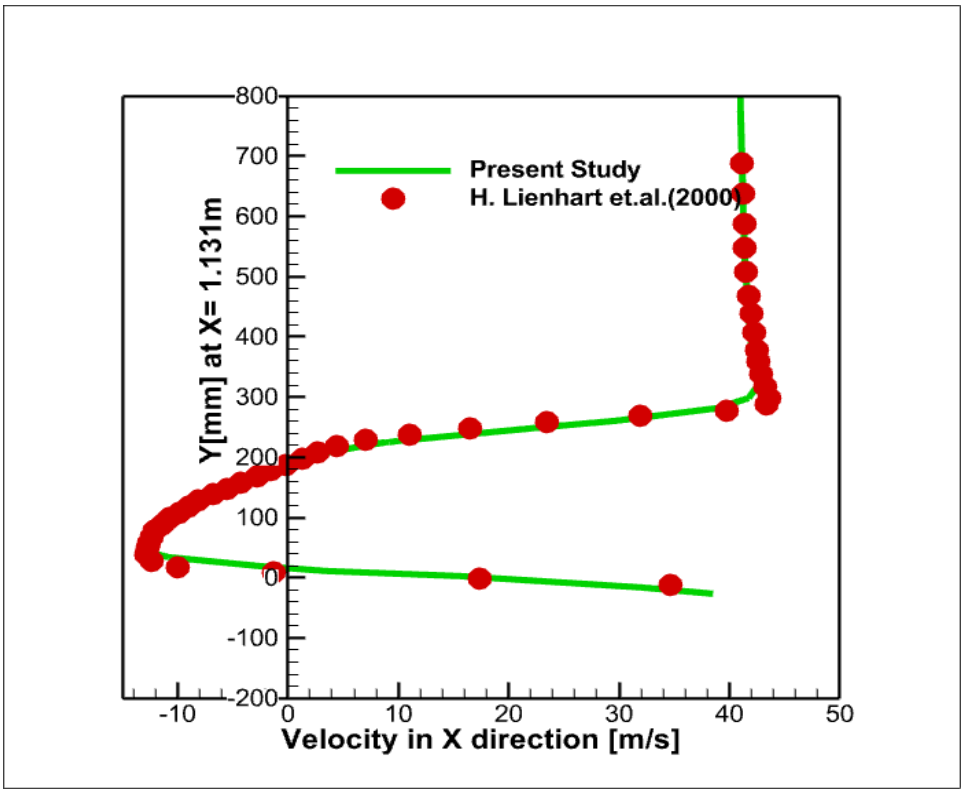
Present Study
H. Lienhart et.al.(2000)
Y[mm] at X= 1.131m
Velocity in X direction [m/s]
800
700
600
500
400
300
200
100
0
-100
-200
-10
0
10
20
30
40
50

(c)

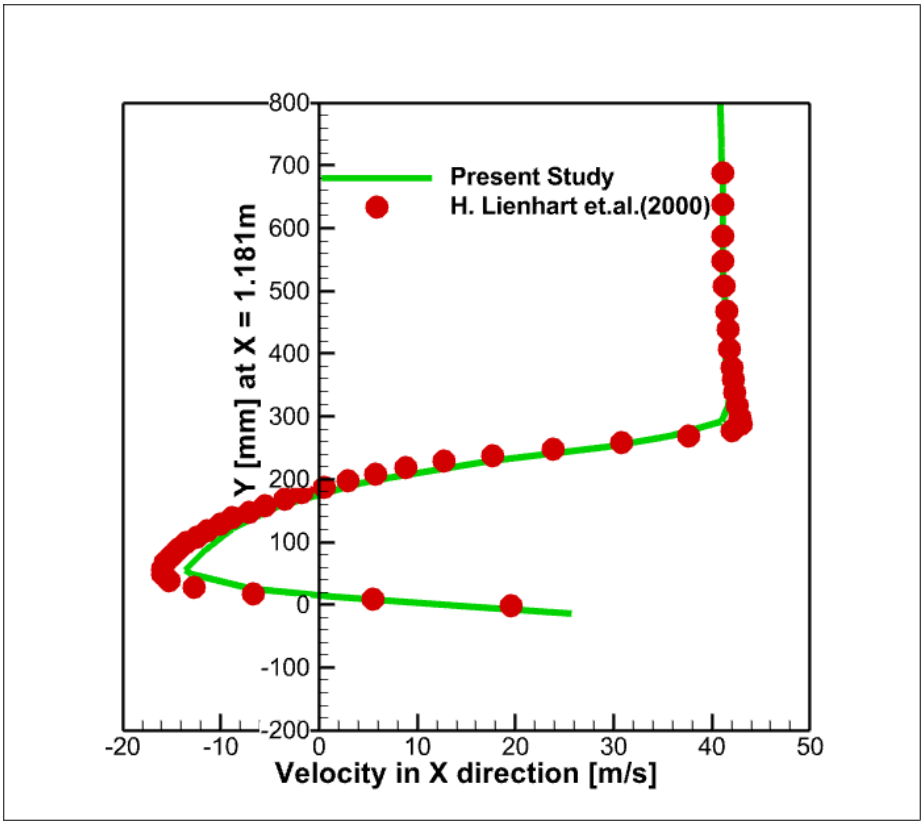

(d)

Fig 4.2 Variation of velocity in x direction along a line (a) x=0.931m (b) x= 0.981m (c) x= 1.131m (d) x= 1.181m.

The above graph is validated with the experimental results done by H.lienhart.et.al in the research article “Flow around a simplified car body (Ahmed body)”.The above four graphs shown in figure are made on symmetry1 plane. The line x= 0.931 and x=0.981m are on the slant surface whereas x=0.131m and x=0.181m are on the wake region. By seeing the above four graphs it is concluded that the flow is separated on these locations as near the slant surface there is a negative component of velocity in x direction.

4.3 Coefficient of Pressure (C_p) Plot at U_∞ = 40m/s and α=35°

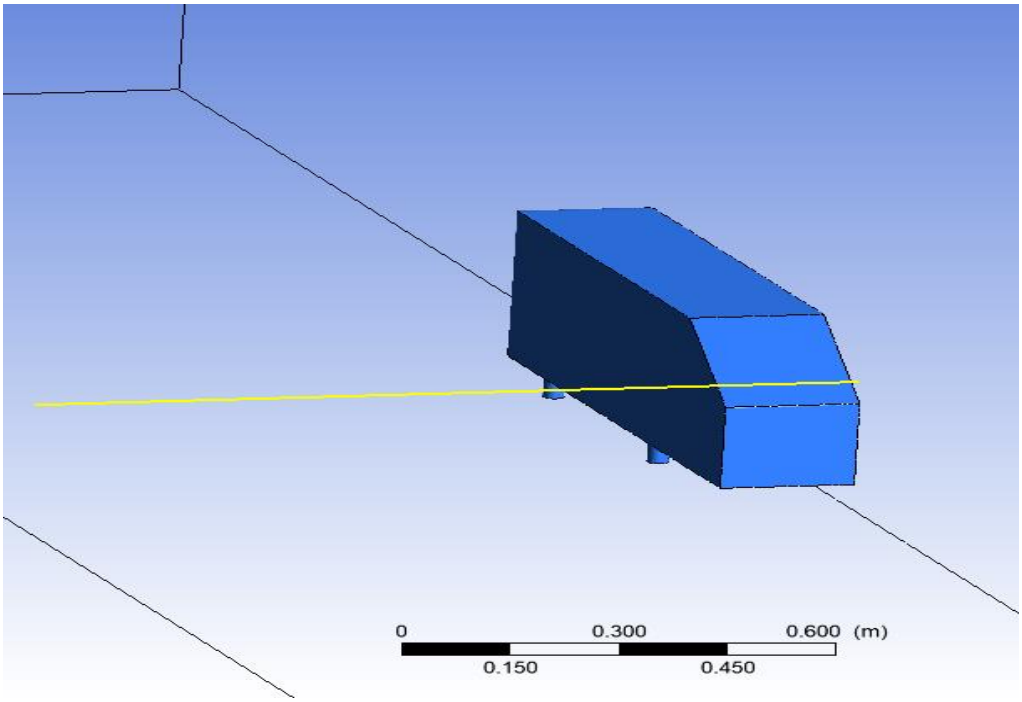

The line has been drawn above the slant surface of Ahmed body at X =1.03 m with different values of Y coordinate like 190.8mm, 260mm, 280 mm. The line is varied along the z axis, on which Coefficient of pressure is plotted. The starting point of the line is at the middle plane of Ahmed body.

The graph is shown below, the variation C_p is shown for half part of Ahmed model. The same variation will be at the other half part of Ahmed model. We can imagine the graph for the full model as if we take reflection about the Y axis of the graph. It can be shown from the graph that from the slant surface, when we go above in the region of wake, the COP at the center of the Ahmed body is increasing.

$$C_p = {(P - P_\infty)}\Big/{(0.5 \times \rho \times U_\infty^2)}$$

Here ρ is the density of air, U_∞ is the free stream velocity, P is the static pressure at the point at which pressure coefficient is being evaluated, P_∞ is the static pressure in the free stream.

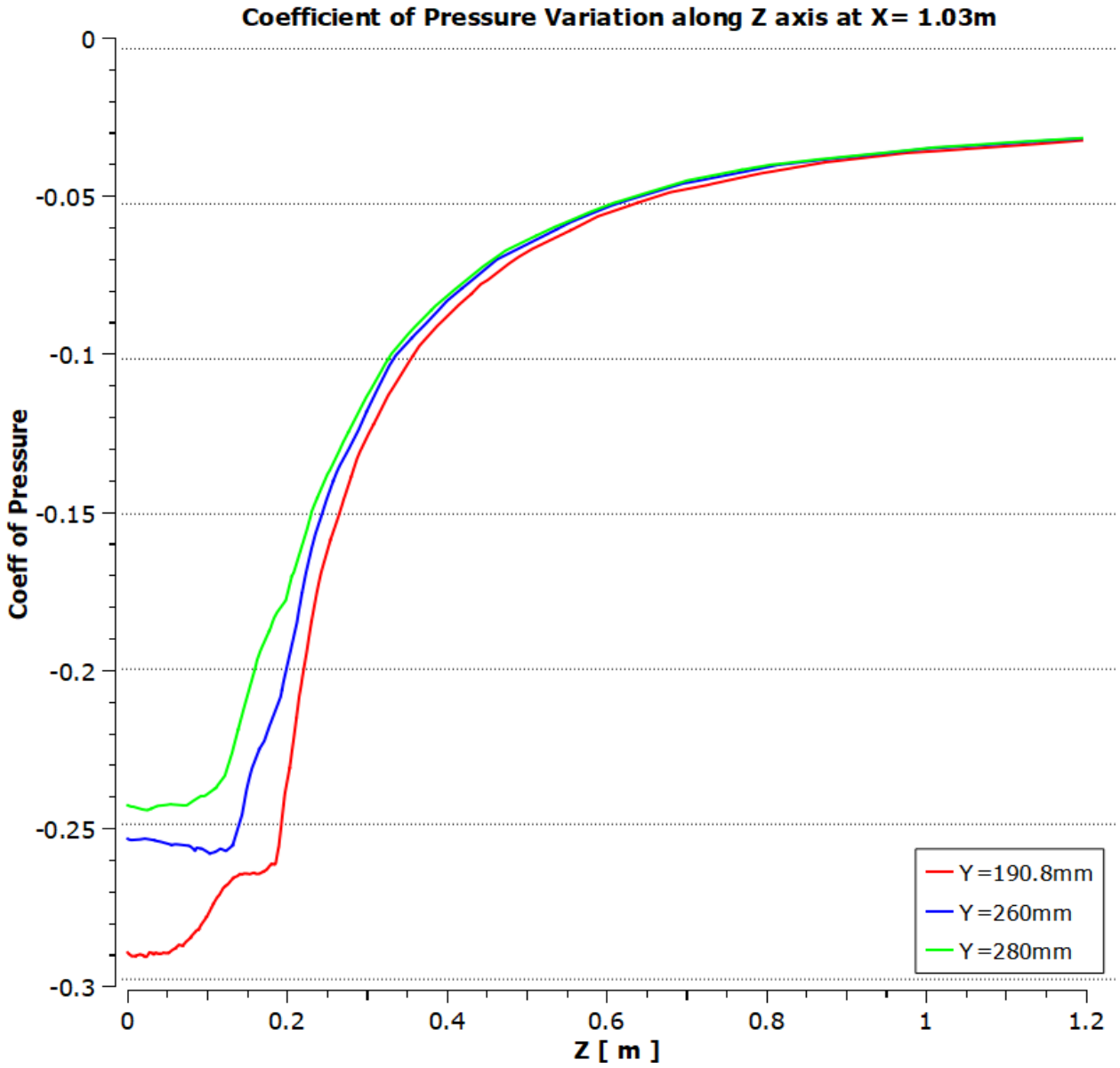

Fig 4.3 Variation of coefficient of pressure along a line Y= 190.8mm, 260mm, 280mm.

4.4 Contour Plots

4.4.1 Velocity Magnitude Contour at U_∞ =30 m/s and α=35°

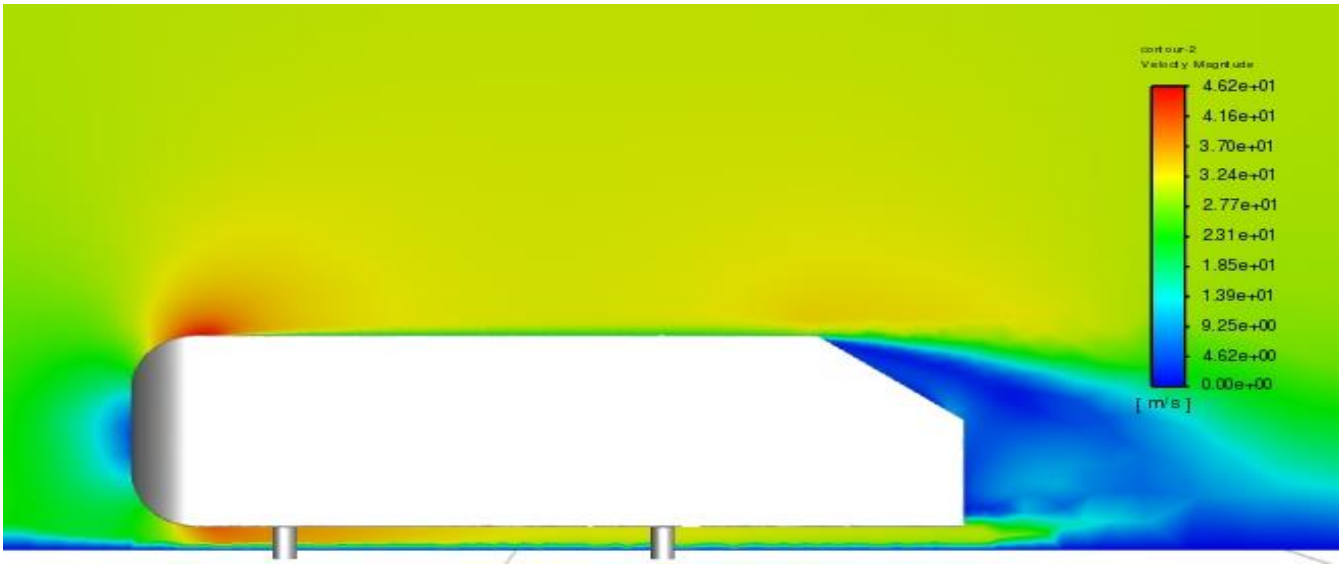

Fig 4.4 Velocity Magnitude Contour at U_∞ =30 m/s and α =35°

For α= 35˚the flow is fully attached at the tip of the roof. At=35 there are two recirculation torus was formed along with a pair c-pillar vortices.

4.4.2 Path lines at U_∞ =30m/s and α= 35˚

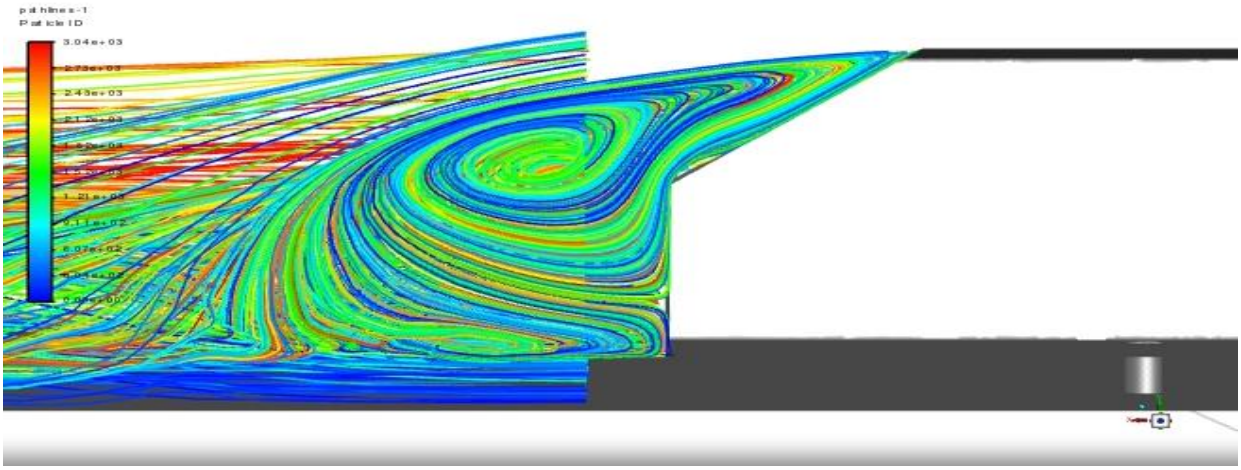

Fig 4.5 Path lines at U_∞ =30 and α= 35˚

When α > 30° , then there is a flow separation starts at the at the tip of the roof of Ahmed body causing two counter- rotating vortices formed on the slant surface and the vertical back of the Ahmed body. This 3d flow over the slant surface weakens the c-pillar vortices due to which overall aerodynamic drag is reduced at slant angle 35˚when compared with 30°

˚

4.4.3 Path Lines at U_∞ = 30m/s and α =30°

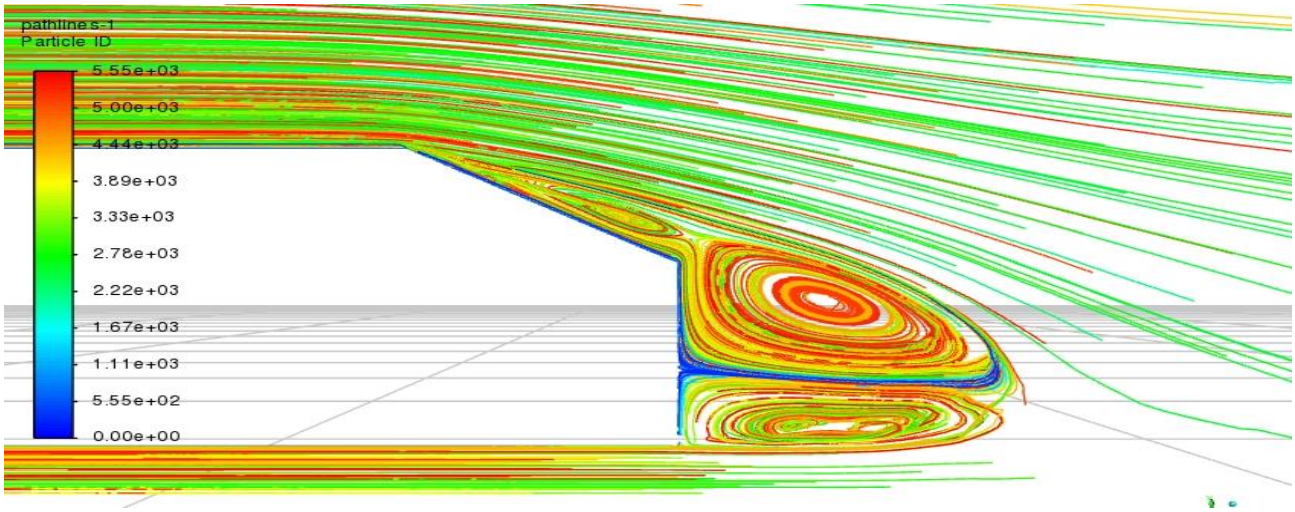

Fig 4.6 Path Lines at U_∞ =30 and α =30°

In case of α =30̊ , there is a flow separation starts at the tip of the slant surface and reattaches in the downstream direction , due to which there is a formation of separation bubble on the slant surface which interact with the c-pillar vortices and make them stronger. This is the region why coefficient of drag suddenly shoot up at α =30°

4.4.4 C-Pillar Vortices at U_∞=30m/s and α = 30°

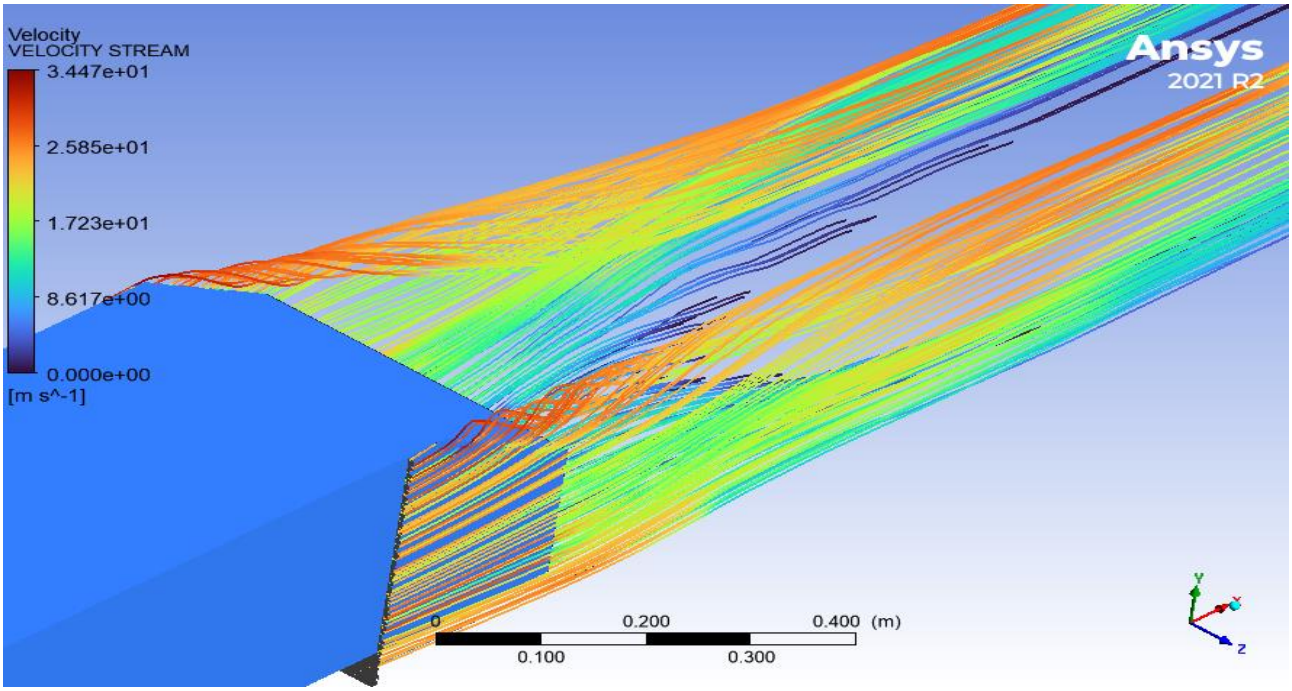

Fig 4.7 Path lines of C-Pillar vortices at U_∞=30 m/s and α =30°

4.4.5 Path Lines at U_∞ = 30m/s and α =25°

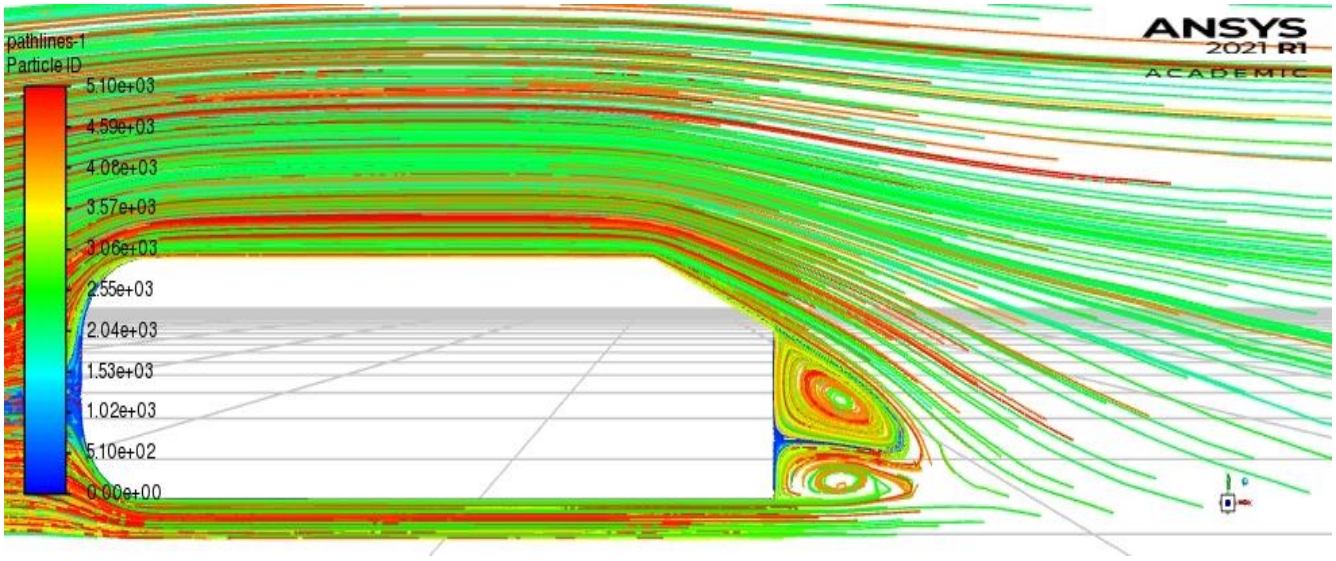

Fig 4.8 Path lines at U_∞ =30 m/s and α= 25°

At α = 25˚ there are two recirculation torus along with c-pillar vortices, here the flow separates at the bottom edge of slant surface. Between α>12.5° and < 30° the flow is attached to the slant surface and the flow behind the Ahmed body becomes more 3 dimensional and the strength of longitudinal vortices also increased in this regime which causes drag to increase.

4.4.6 Pressure contours behind the Ahmed body at x= 1.3m for U_∞= 30m/s and α=30°

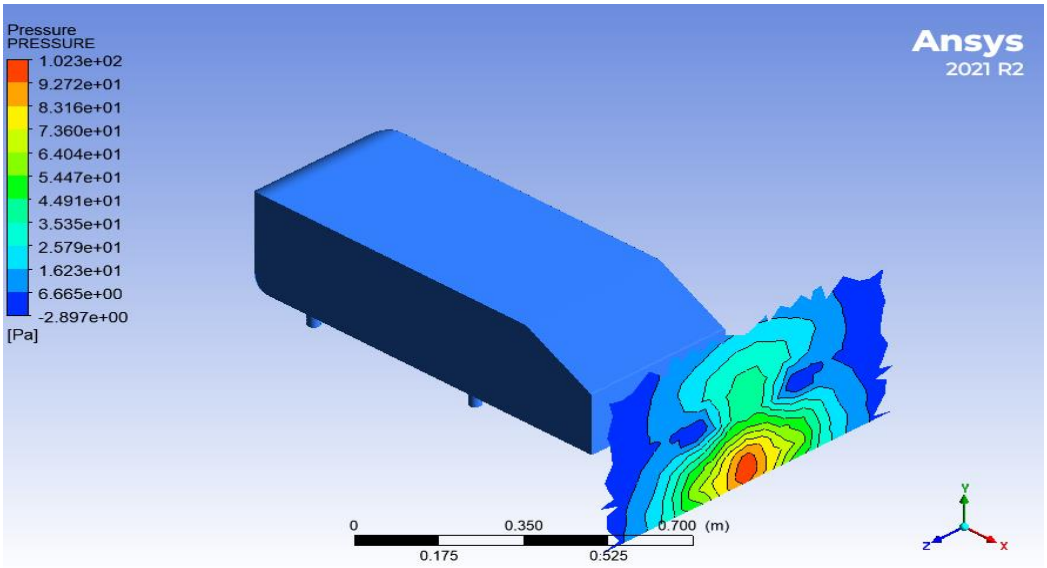

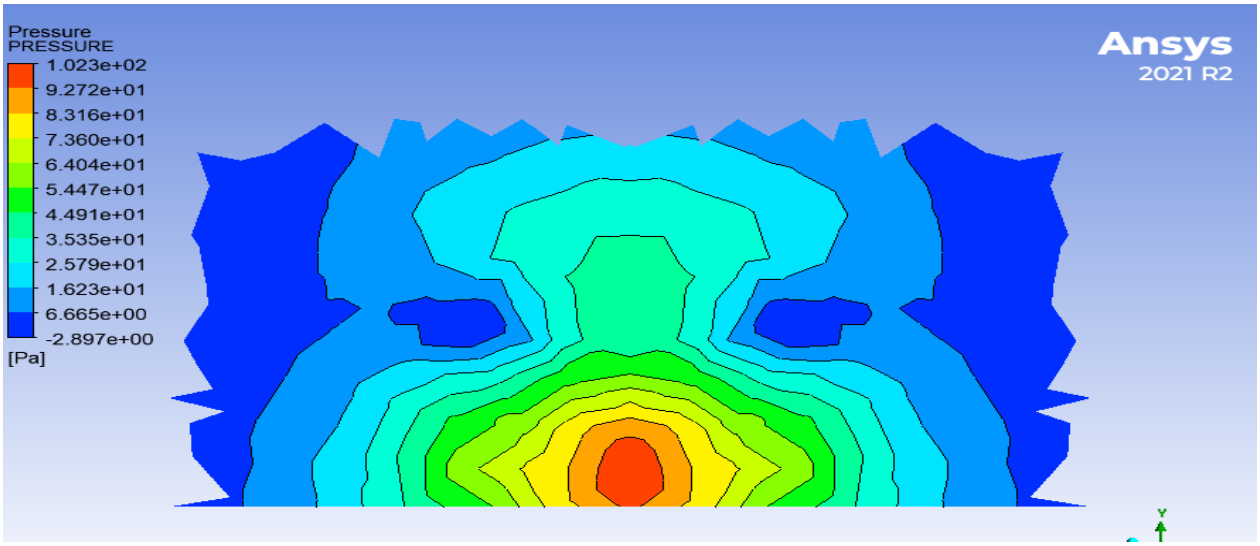

(a)

4.4.7 Pressure contours behind the Ahmed body at x= 1.3m for U_∞ = 30m/s and α=35°

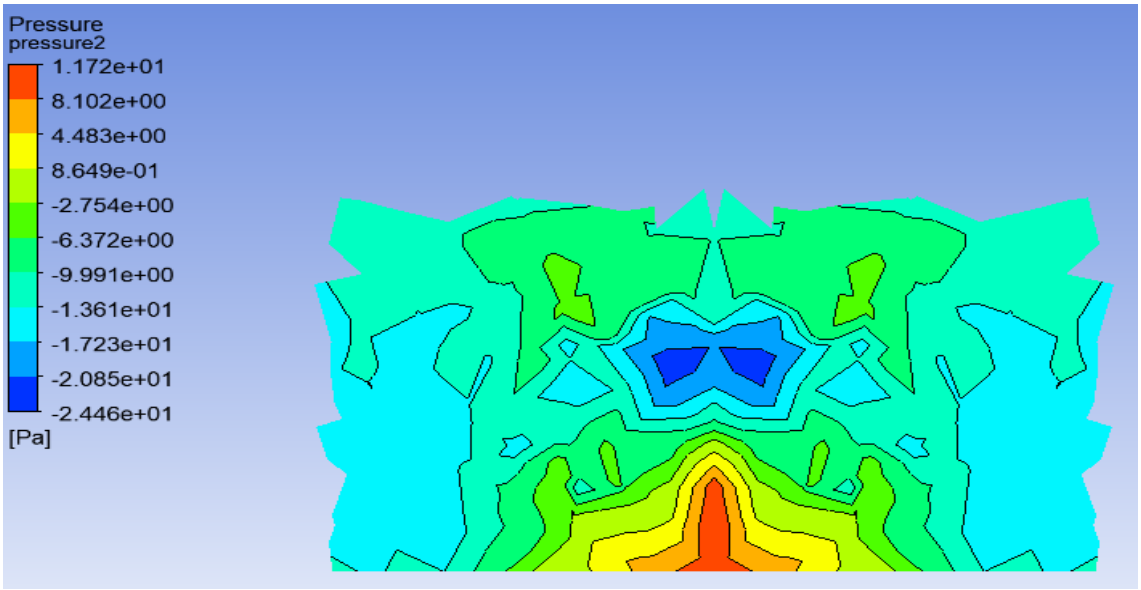

(b)

Fig 4.9 Pressure contours behind the Ahmed body at x= 1.3m for U_∞=30 and (a) α=30˚

(b) α=35˚

While comparing the plots for α=35° and 25°, it can be concluded that the pressure recovery is better for the case when back slant angle is 35°. It can also observed the intensity of the eddies in case of 25 degree back slant angle is more than the 35°case and those eddies are more far as compared to near eddies. Hence the drag coefficient is more for α=25°. Also due to lower size of eddies in case of 35 degree back angle it means rate of kinetic energy dissipation in plane x= 1.3m when compared with 25 degree back angle

4.4.8 Turbulent Kinetic energy contour for U_∞ = 30m/s and α =30°

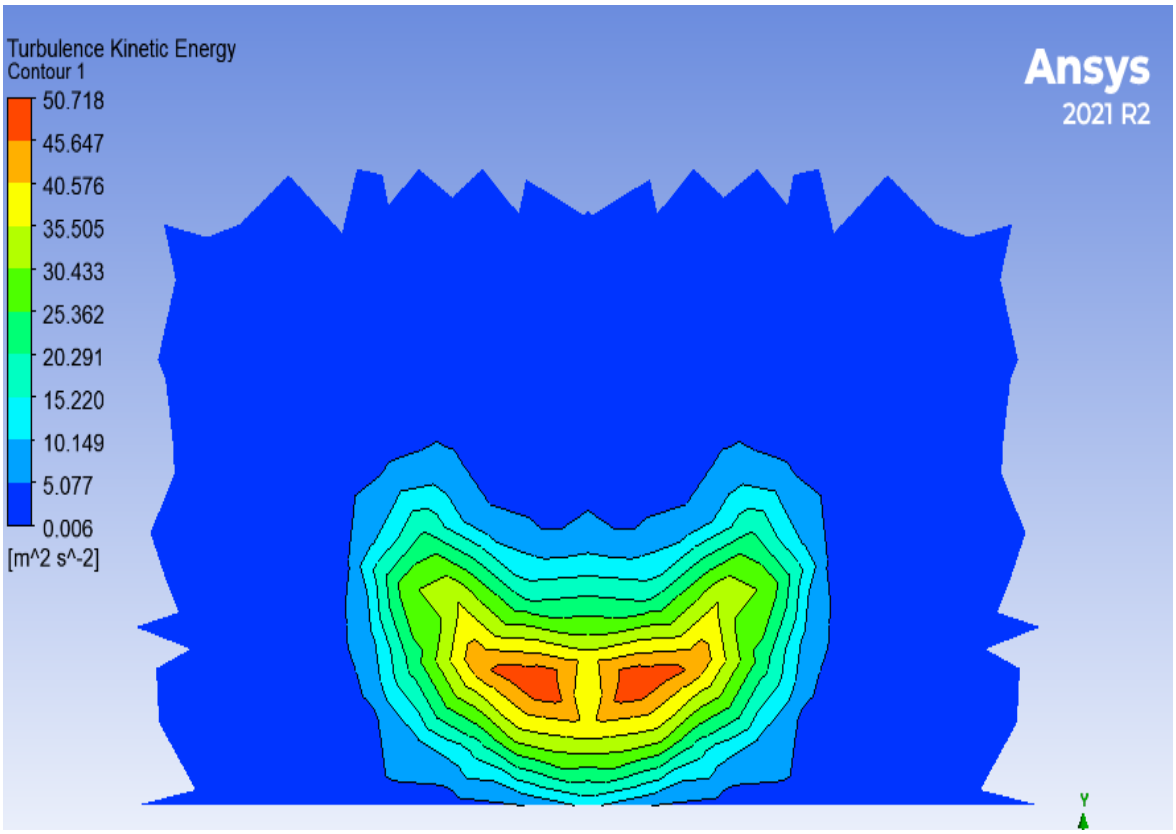

(a)

4.4.9 Turbulent Kinetic energy contour for U_∞= 30m/s and α =35°

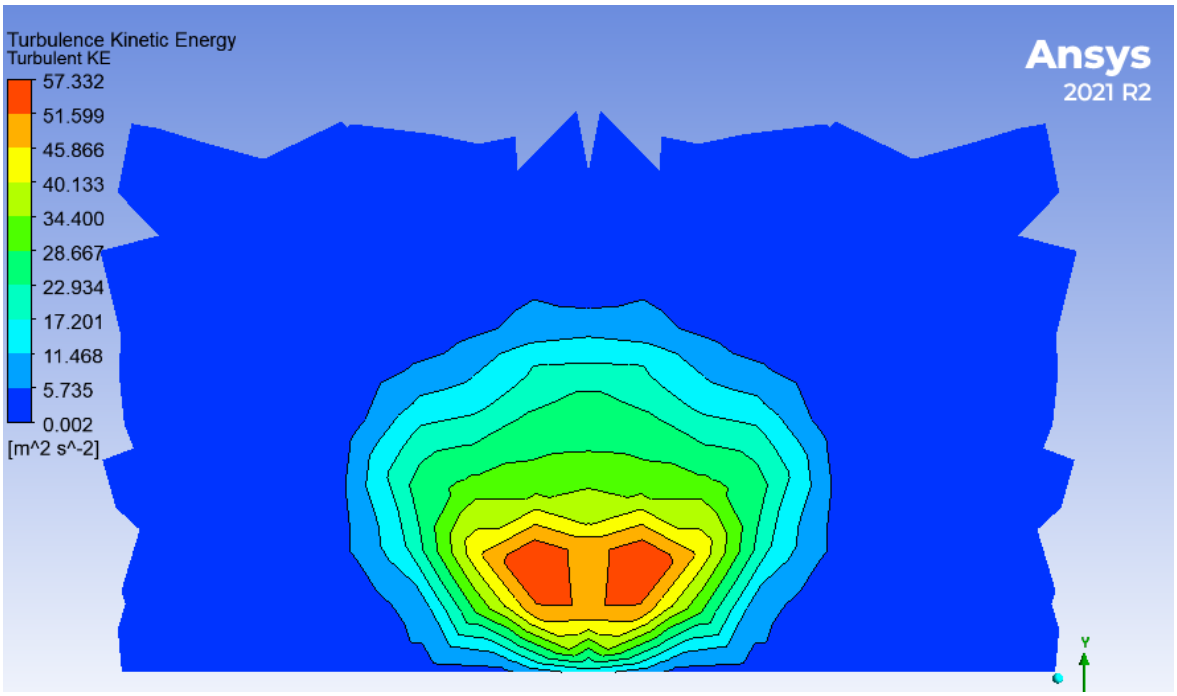

(b)

Fig 4.10: Turbulent kinetic energy for U_∞ = 30m/s and (a) α= 30˚, (b) α=35˚

Turbulent kinetic energy is the energy associated with the eddies in a turbulent flow. For the continuous circular motion of these eddies requires energy , that energy was extracted from the mean flow in a near region Firstly the kinetic energy of the mean flow was transferred to the largest eddies and from larger eddies the energy was transferred to the smaller eddies and finally when viscous effect dominant compared with inertia effect , the energy is going to dissipate in very small eddies. Larger the size of an eddy larger will be the turbulent kinetic energy associated with that eddy. By comparing the turbulent kinetic energy for the back slant angle 30° and 35° at free stream velocity of U_∞ = 30 m/s , it was clearly observed that at x= 1.3 plane Turbulent Kinetic energy is more for α =35° when compared with α =30° . it means the loss ok kinetic energy from the mean flow in order to continue the eddies is more for α =35°.

4.4.10 Momentum source term magnitude contour for plasma actuator at 35° and U_∞ =30 m/s

(Momentum Source or Plasma source = 10000 N/m^3)

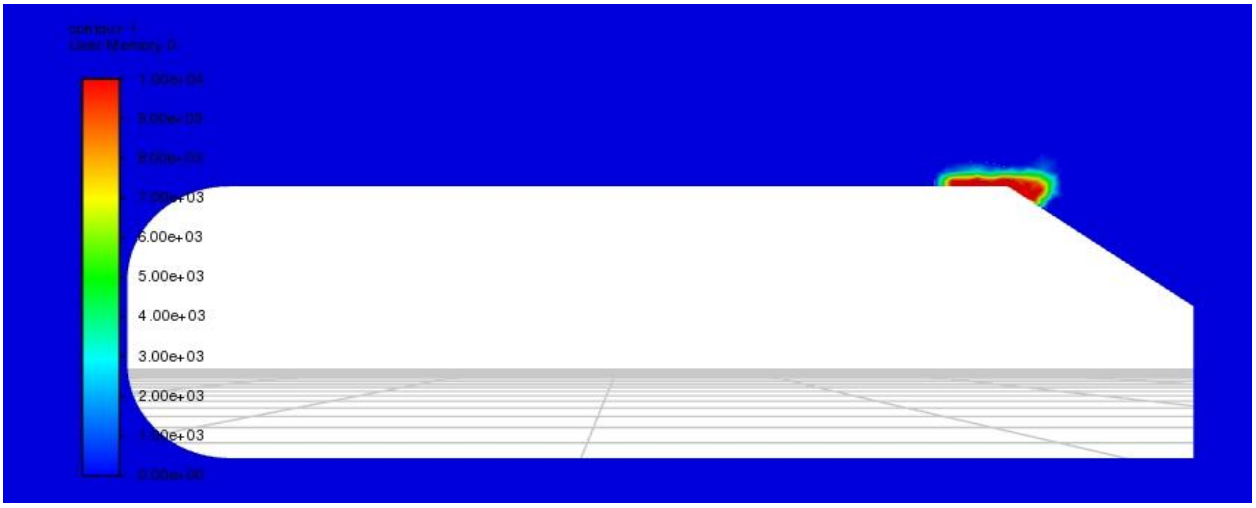

Fig 4.11 Contour plot for location of Plasma actuator

As the study shows that the location of plasma actuator is effective where the flow separation occurs in a car model. The above figure shows the location of plasma actuator with thickness 12 mm and length 100 mm .This is the region where momentum source term is applied. The momentum source term value which is equivalent to body force equals to 10000 N/m^3 is applied to see the variation of velocity profile.

4.4.11 Velocity Magnitude contour for plasma actuator at 35° and U_∞ =30 m/s

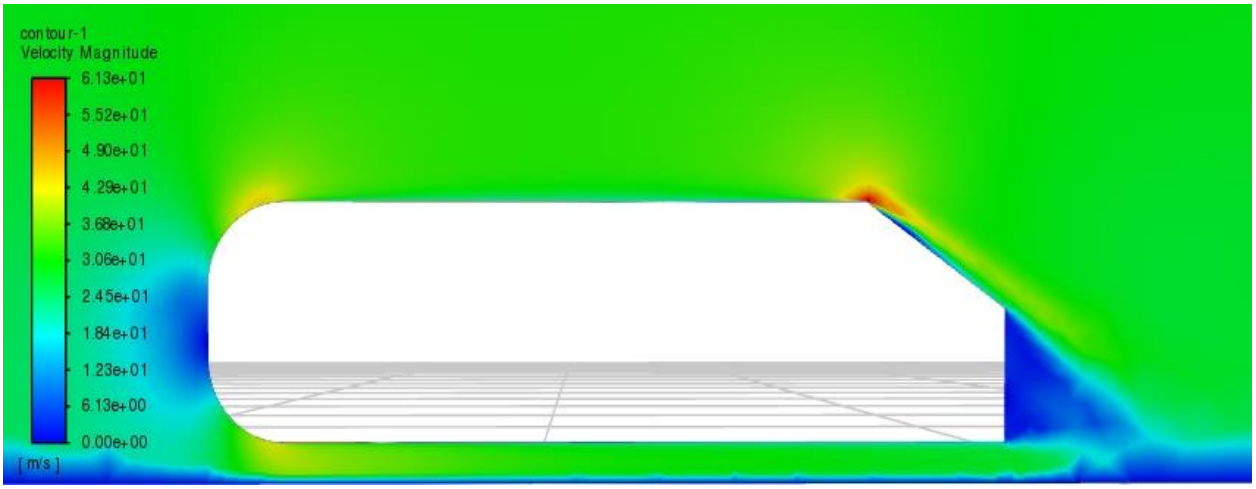

Fig 4.12 Velocity Magnitude contour for plasma actuator at α= 35° and U_∞ =30 m/s

The figure shown above is the contour for velocity profile with plasma actuator, It can be seen from the graph that the wake zone is minimized due to high velocity of air particle above the slant surface, we can see that there is no flow separation happen on the slant surface. As the drag coefficient is the combination of pressure drag and friction drag. Due to the flow separation at various location in rear of the car like tip of the roof, c-pillar, vertical back surface of Ahmed body, it creates a negative pressure behind a car due to which the difference between the front and rear pressure of the car increases and hence pressure drag increases. The main component of aerodynamic drag is mainly pressure drag. Here due to high velocity of air at the slant surface, the pressure in this region is decreases, due to which there is high pressure difference between the front and back side of the body. In the above case where the plasma source term value is equals to 10000 N/m^3, the drag coefficient is increased ,which shows that the flow structure behind the car doesn't improve by employing plasma actuator with this high value of plasma source term. Hence by manipulating the thickness, length of the plasma region with body force term value, we can find the optimum region which helps in overcoming or delaying the flow separation at the slant surface so that coefficient of drag will be reduced.

4.4.12 Vector Plot at U_∞ =30 and α =35 with Plasma Actuator

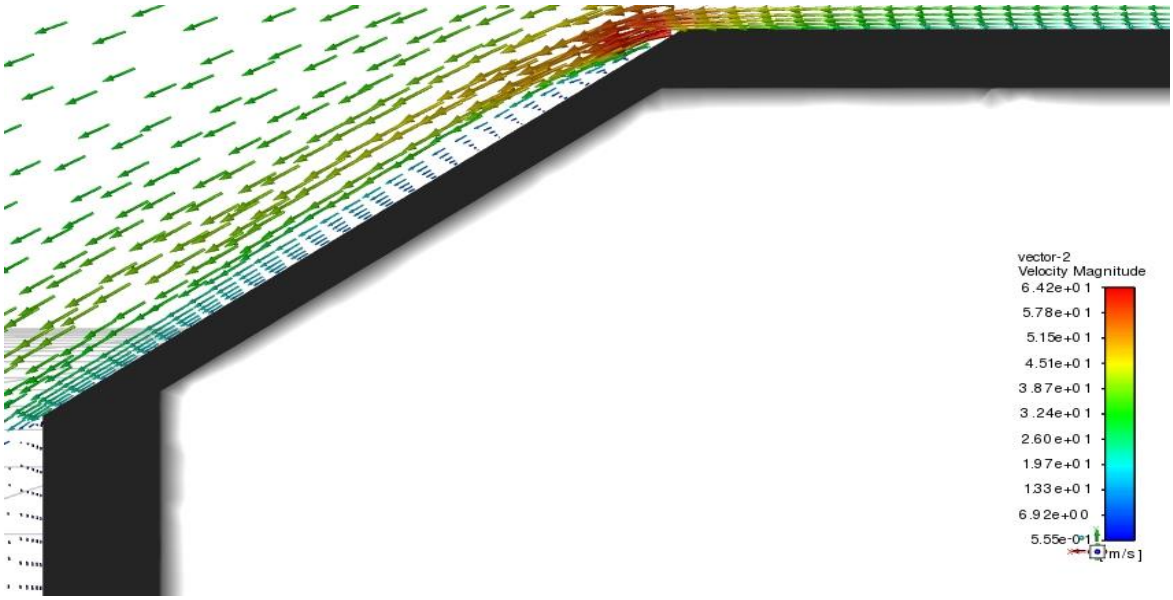

Fig 4.13 Vector Plot at U_∞ =30 and α =35˚with Plasma Actuator

The below table shows the Pressure coefficient and viscous coefficient breakdown for the above case

	Pressure Coefficient	Viscous Coefficient	C_d
Without Plasma	0.24618	0.04749	0.29367
With Plasma	0.34933	0.05398	0.40331

TABLE 4.2 Breakdown of Pressure Coefficient and Viscous Coefficient for Plasma source = 10000 (N/m^3)

From the above observation it can been seen that due to high value of plasma source term equals to 10000 N/m^3, there is increase in both pressure and viscous coefficient. Hence there is a need of optimization of region of plasma actuator with varying the plasma source term value.

4.4.13 Pressure contours for both without Plasma and with Plasma behind the Ahmed body at x= 1.3m for U_∞ = 30 and α=35°

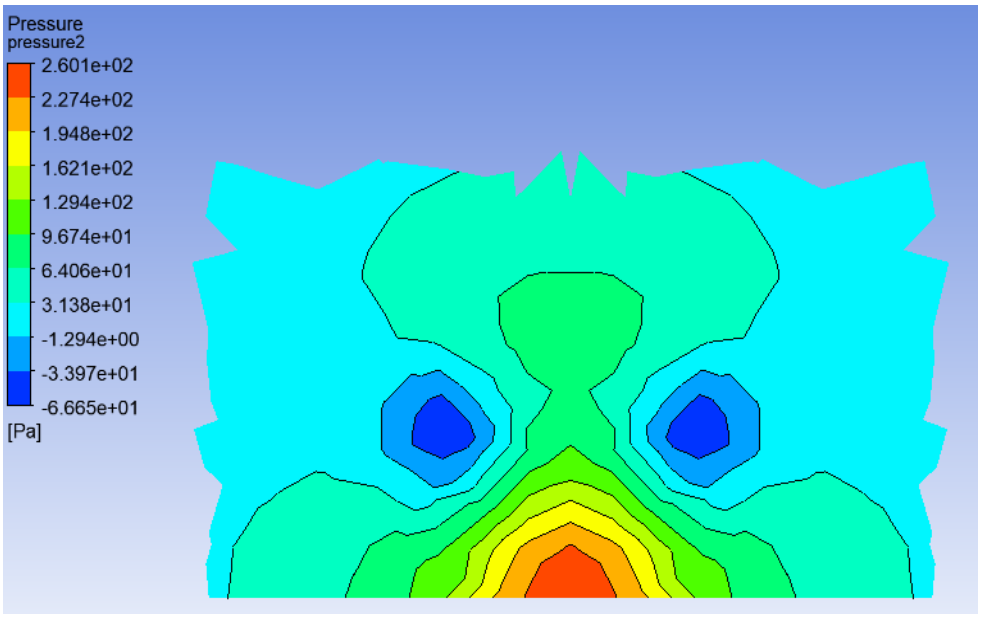

With Plasma

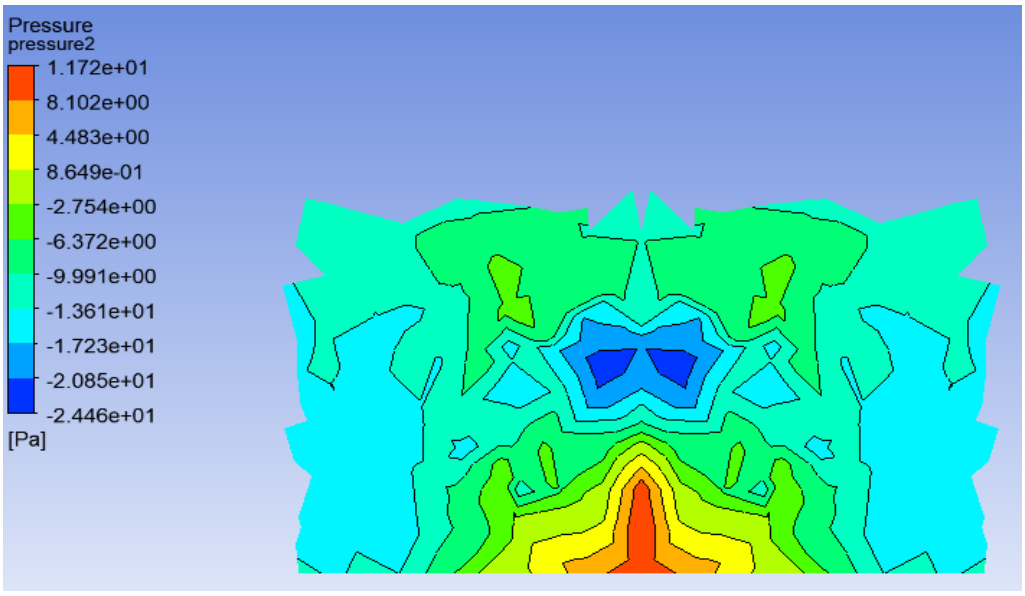

Without Plasma

Fig 4.14: Pressure contours for both without Plasma and with Plasma behind the Ahmed body at x= 1.3m for U_∞ = 30 and α=35˚

It can be seen from the graph that with plasma actuator on the model changes the flow structure behind the car. The pressure distribution at the back side of car without plasma is more uniform

and pressure recovery is better than the with plasma actuator model which helps to reduce the pressure drag of the car. For the pressure contour plot in case of with plasma, it can be observed that the intensity of induced vortices are high and they are apart from a certain distance when compared with contour plot of without plasma. These are the reason why drag coefficient increases.

4.5 Coefficient of Pressure with and without Plasma Actuator at α=35˚ and U_∞ =30m/s

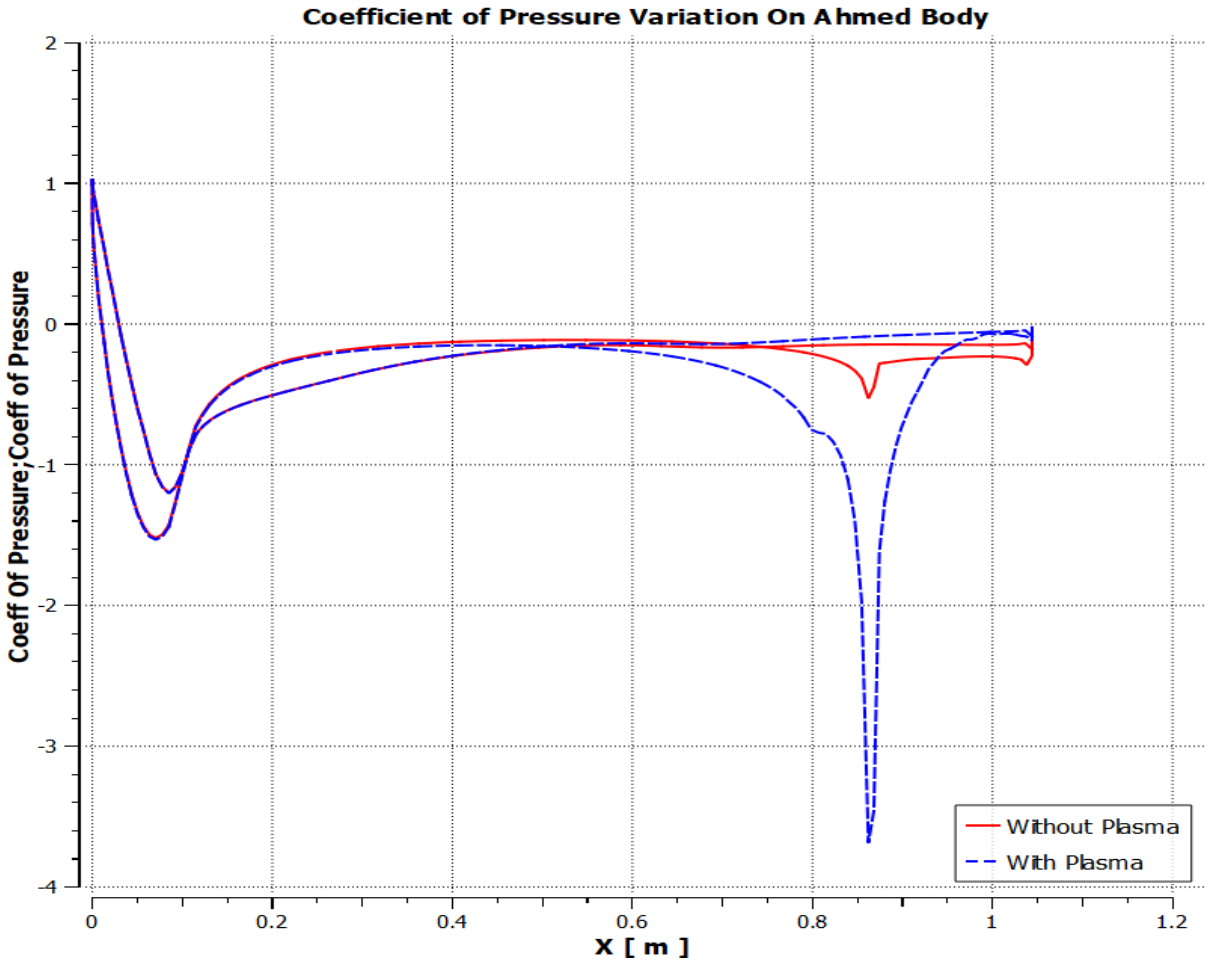

Fig 4.15: Variation of C_P with and without Plasma actuator at α=35˚ and U_∞ = 30m/s

The C_P variation over Ahmed body with plasma actuator with plasma source term value equals to 10000 N/m^3 is shown in above figure. It is compared with the cop variation when there is no plasma actuator. It can be seen from the graph that pressure drops suddenly at the slant surface due to which the major term in drag coefficient known as pressure drag increases

Comparison of Aerodynamic drag for different thickness of plasma region at u=30m/s and α =35°

S.NO	PLASMA SOURCE (N/m^3)	THICKNESS(mm)	C_d
1	NO	0	0.2936
2	100	2mm	0.2818
3	150	2mm	0.2937
4	100	1mm	0.2925

TABLE 4.3 Comparison of Aerodynamic drag for different thickness of plasma region at u=30m/s and α =35°

In this study the plasma region length is remained constant which is equals to 70mm and the thickness of the plasma region is varied with the different values of plasma source value.

The below Table 4.4 shows the comparison of Pressure Coefficient and Viscous Coefficient for the two cases with and without Plasma employed on 35° degree back angle Ahmed body. These cases are shown in Table 4.3 with S.No 1 and 2.The data for different coefficients are shown below:-

	Pressure Coefficient	Viscous Coefficient	C_d
Without Plasma	0.24618	0.04749	0.29367
With Plasma	0.23286	0.04898	0.2818

Table 4.4 Comparison of Pressure coefficient and Viscous Coefficient with Plasma source =100 (N/m^3)

From the above observation it is find that with the help of Plasma source term, the pressure coefficient is decreased whereas the viscous coefficient is increased. This is due to the addition of momentum to fluid particles near the separation zone which is at the tip of the roof. As I near the tip of the slant surface where the plasma actuator model is mounted, there Is sudden increase in velocity of fluid particle due to which viscous shear over the Ahmed body increases which causes viscous coefficient to increase.

4.6 Plasma actuator modeled vertical back surface

4.6.1 Contour Plot of momentum source term on the vertical back edge behind the Ahmed body

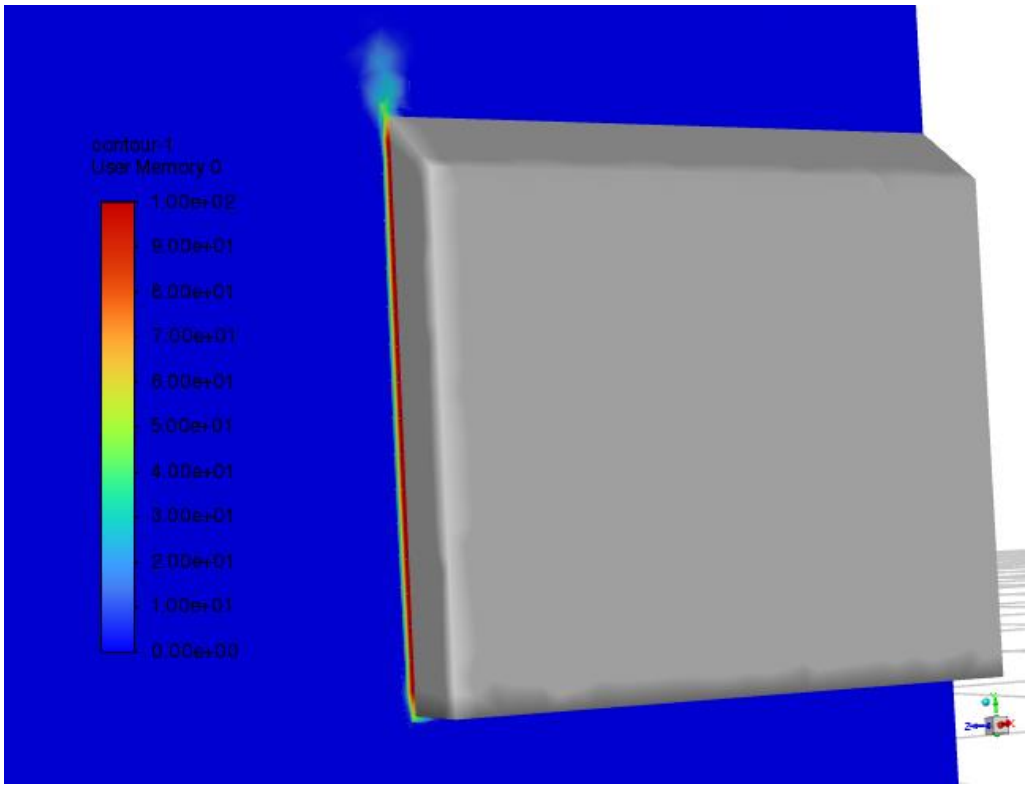

Fig 4.16 Location of Plasma region at vertical surface on back side of Ahmed Body.

Here the plasma actuator is modeled on the vertical back surface to see the effect on drag coefficient. The optimization has been done to find out the suitable region for plasma actuator.

S.NO	PLASMA SOURCE (N/m^3)	LENGTH(mm)	THICKNESS(mm)	C_d
1	NO	0	0	0.2936
2	100	70	2mm	0.2981
3	200	50	3mm	0.2937
4	500	50	3mm	0.2765

TABLE 4.5 Optimization of location of plasma actuator on vertical back surface of Ahmed Body

4.7 Plasma actuator modeled on both tip of the slant edge and at the vertical back surface

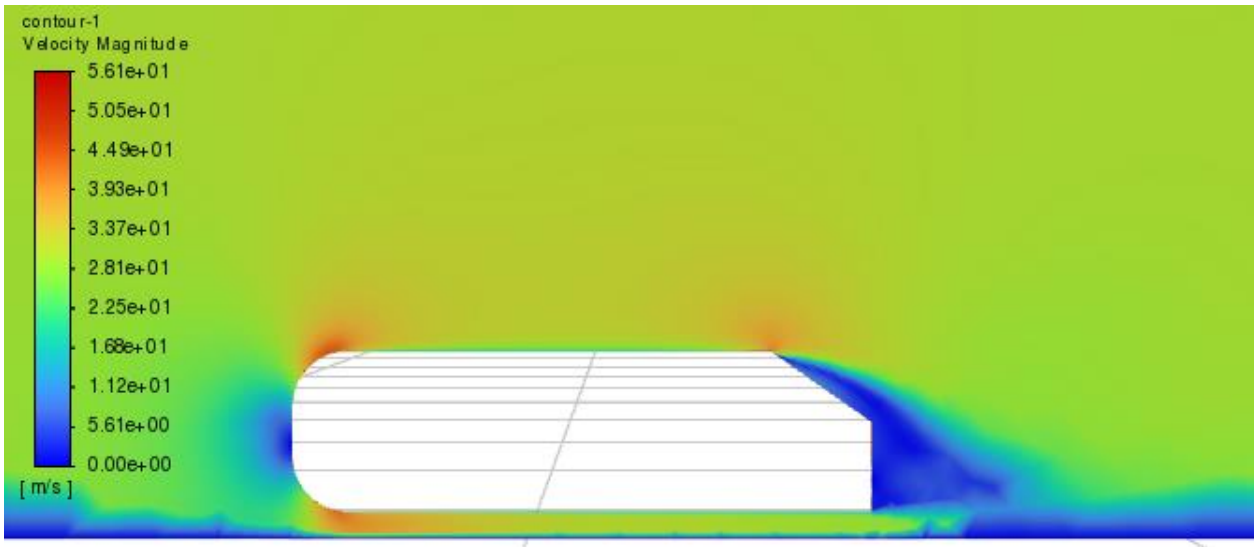

Fig 4.17: Velocity Magnitude Contour plot for Plasma on both surface

The combination of plasma region on upper edge of roof and lower vertical edge of Ahmed body from backside was employed to see drag coefficient variation at 35° back angle and it was evaluated that for 3mm thickness and 70mm length of plasma region with momentum source term equals to 1000 N/m^3, the aerodynamic drag is increased from 0.29367 to 0.29821

	Plasma Source(N/m^3)	Pressure Coefficient	Viscous Coefficient	C_d
Without Plasma	NO	0.24618	0.04749	0.29367
With Plasma	1000	0.25044	0.04776	0.29821

TABLE 4.6 Comparison of Pressure coefficient and Viscous Coefficient with Plasma source =1000 N/m^3 on vertical back surface of Ahmed Body

APPENDIX A

PLASMA ACTUATOR UDF

This is the UDF code used at the tip of the roof surface with source term is equals to 1000.0

```
#include "udf.h"

DEFINE_SOURCE(plasma_source, c, t, dS, eqn)
{
#if !RP_HOST
        real xc[ND_ND];
        real source, x, y,z;

        C_CENTROID(xc, c, t);
        x = xc[0];
        y = xc[1];
        z = xc[2];
#if RP_NODE
        if ((x > 0.77) && (y > 0.28) && (z > 0) && (x < 0.85) && (y < 0.3) && (z < 0.1945))
        {
                source = 1000.0;
                dS[eqn] = 0;
        }
        else
        {
                source = 0;
                dS[eqn] = 0;
        }
        C_UDMI(c, t, 0) = source;
#endif
        return source;
#endif
}
```